Bachelor Thesis

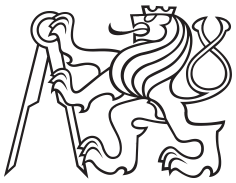

Czech Technical University in Prague

F3

Faculty of Electrical Engineering
Department of Control Engineering

Vehicle Slip Ratio Control System for Torque Vectoring Functionality

Petr Turnovec

Supervisor: Ing. Haniš Tomáš, Ph.D.
Field of study: Cybernetics and Robotics
May 2019

BACHELOR'S THESIS ASSIGNMENT

I. Personal and study details

Student's name: **Turnovec Petr** Personal ID number: **459919**

Faculty / Institute: **Faculty of Electrical Engineering**

Department / Institute: **Department of Control Engineering**

Study program: **Cybernetics and Robotics**

II. Bachelor's thesis details

Bachelor's thesis title in English:

Vehicle slip ratio control system for torque vectoring functionality

Bachelor's thesis title in Czech:

Řízení podelného skluzu kol vozidla pro systém rozdělení trakčního momentu

Guidelines:

The goal of the thesis is follow-up development of vehicle traction control system, namely the development and implementation of torque vectoring control algorithms in Matlab & Simulink environment. The main objective is torque vectoring system development based on slip ration control algorithms. This is very challenging task dealing with highly non-linear dynamics and time variant system. Results will be validated based on virtual verification environment and using driver on board platform, in cooperation with eForce Formula student. Results are essential for the further vehicle control system design development.
1. Get familiar with vehicle dynamics single track and twin track models, tier models. Adoption of such models for purposes of thesis algorithms development and verification.
2. Traction algorithms development.
3. Algorithms verification on simulation based environment.
4. Algorithms verification based on drive tests.

Bibliography / sources:

[1] Edward M. Kasprzak, L. Daniel Metz, William F. Milliken Douglas L. Milliken, Race Car Vehicle Dynamics - Problems, Answers and Experiments, Premiere Series Books, 2015, ISBN-10: 0768011272.
[2] Prof. Dr.-Ing. Uwe Kiencke Prof. Dr. Lars Nielsen; Automotive Control Systems, Springer, 2005
[3] Denis Efremov, Unstable ground vehicles and artificial stability systems, 2018
[4] Marek Laszlo, Flight Control Solutions Applied for Improving Vehicle Dynamics, 2019

Name and workplace of bachelor's thesis supervisor:

Ing. Tomáš Haniš, Ph.D., Department of Control Engineering, FEE

Name and workplace of second bachelor's thesis supervisor or consultant:

Date of bachelor's thesis assignment: **01.02.2019** Deadline for bachelor thesis submission: **24.05.2019**

Assignment valid until:
by the end of summer semester 2019/2020

Ing. Tomáš Haniš, Ph.D.	prof. Ing. Michael Šebek, DrSc.	prof. Ing. Pavel Ripka, CSc.
Supervisor's signature	Head of department's signature	Dean's signature

III. Assignment receipt

The student acknowledges that the bachelor's thesis is an individual work. The student must produce his thesis without the assistance of others, with the exception of provided consultations. Within the bachelor's thesis, the author must state the names of consultants and include a list of references.

. _____
Date of assignment receipt

_____
Student's signature

Acknowledgements

First, I would like to thank my supervisor Ing. Tomáš Haniš, Ph.D. for his valuable advice and supportive supervision of my work.

Great thanks also belong to formula student electric team eForce FEE Prague Formula. I namely thank Ing. Marek László for his drive tests participation and his willingness.

My thanks also belongs to Ing. Denis Efremov for his helpful advice.

Last, yet the most, I would like to thank my family for their support.

Declaration

I hereby declare that this bachelor's thesis was finished on my own and that I have cited all the used information sources in compliance with the Methodical guideline on the observance of ethical principles in the preparation of university graduate thesis.

In Prague, 20 May 2019

Abstract

This thesis deals with control system development for torque vectoring functionality on vehicle rear axle. At first mathematical model of vehicle and its tires is introduced. Then vehicle stability, understeering and oversteering is analyzed. Further on the brief vehicle behavior analysis is described. Control algorithms improving vehicle dynamics are developed by method named model based design. The thesis is focused on two main approaches to their design. The first one is standard symmetrical torque vectoring on rear axle. The second one extend the first one with longitudinal slip ratio control. There are presented test results in simulation environment and drive test results verified on functional student electronic formula car at the end of the thesis.

Keywords: torque vectoring, longitudinal slip ratio, vehicle dynamic, control system, understeering, oversteering, formula student electric

Supervisor: Ing. Haniš Tomáš, Ph.D.

Abstrakt

Tato práce se zabývá vývojem řídících systémů pro rozdělování hnacího momentu na kola zadní nápravy vozidla. Nejprve je představen matematický model vozidla a jeho kol. Pak je rozebírána stabilita vozidla, jeho nedotáčivost a přetáčivost. Následně je podána krátká analýza chování vozidla. Na základě modelu jsou pak vyvinuty řídící algoritmy zlepšující dynamiku vozidla. Práce se věnuje především dvěma přístupům k jejich návrhu. Prvním je běžný způsob rozdělování momentů symetrickým způsobem. Druhý přístup rozšiřuje první o kontrolu podélného prokluzu kol. Závěrem jsou prezentovány výsledky testů v simulačním prostředí a jízdních testů provedených na studentské formuli.

Klíčová slova: rozdělování hnacího momentu, podélný skluz, dynamika vozidla, řídící systém, nedotáčivost, přetáčivost, studentská elektrická formule

Překlad názvu: Řízení podelného skluzu kol vozidla pro systém rozdělení trakčního momentu

Contents

Figures

Chapter 1

Introduction

Development in last few years in automotive industry opens new possibilities, which bring positive impact on driver and vehicle safety as well as on its control. The opportunity to drive each wheel separately offers engineers in this industry new ways to deal with vehicle behavior. Motors of electric vehicle are more agile. Electric motor in vehicle has faster reaction than classic combustion motor. This development gives an opportunity for invention new control systems. Well known and in vehicle frequently used algorithms are Anti-lock braking system (ABS) and Electronic stability program (ESP). In electric vehicle it is simple to implement traction control systems, its component can also be torque vectoring technology. All of these algorithms aim to stabilize the vehicle or improve its dynamic.

In this thesis the relatively new technology named torque vectoring is examined. Algorithms development is based on method named model based design. It requires vehicle and it's tires mathematical model derivation. Various vehicle behavior analyses will be performed on this model. Developed algorithms will be tested on student formula in cooperation with eForce FEE Prague Formula at the end, with regards to it analyses will be carried out for model parameters matching formula parameters. Then proposed algorithms will work fundamentally as well on other vehicles, but controllers parameters and other values will be valid only for chosen vehicle (formula).

The main aim of this thesis is development and comparison of two control algorithms for torque vectoring functionality. Both of these algorithms will try to modify vehicle lateral dynamics, but one of them will be based on longitudinal slip ratio control and will prevent vehicle tires from undesirable

longitudinal slip. So vehicle should be easier to handle.

Further, front wheels steering angle control options are briefly mentioned. Thus driver don't steer the steering angle of wheels directly, but through steering wheel angle gives request for vehicle cornering. This technology is linked with torque vectoring functionality in this work and then it is compared with algorithm based only on torque vectoring.

The thesis is divided into several chapters. Chapter 2 handles vehicle modeling. Vehicle nonlinear model is adopted and modified. Then one tire modeling approach is described. Further, differences between understeering, oversteering and neutral vehicle are defined in Chapter 3 and brief analysis of formula model is performed. There are proposed control algorithms improving vehicle dynamics in Chapter 4. Chapter 5 shows test results in simulation environment and Chapter 6 then student formula test drive results. Conclusion is presented and future work is outlined in Chapter 7.

1.1 Active Vehicle Control Systems

Torque Vectoring

Torque vectoring (TV) technology tries to improve vehicle dynamics and its stabilization and prevent from critical situations occurrence. This technology importance increases especially with electric vehicle development as each of the wheels can be powered with its own separate motor.

Torque vectoring distribute driving torque to individual wheels. In form of steering wheel angle and accelerator amount we obtain demand for longitudinal and also lateral acceleration. Then system TV affects vehicle dynamics giving different driving torques on individual wheels. It helps the driver to reduce his effort for vehicle steering. TV principle of work is on Figure 1.1.

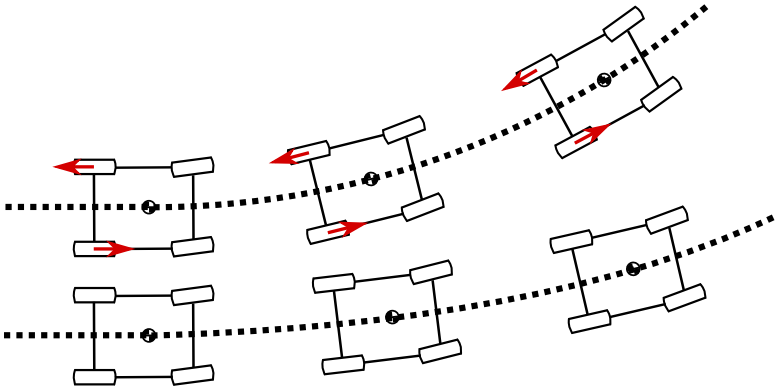

Figure 1.1: TV working on rear axle. Torques difference on rear wheels is indicated by red arrow.

- **Electronic Stability Program**

  The aim of TV is to prevent critical situations, but it is not designed to handle the situation. The main reason are driving torques limitations as torques usually can't be negative. In this situation vehicle control is taken by Electronic stability program (ESP). Principle of its function is same as for TV. But ESP deals with brakes and control breaking torques on individual wheels.

- **Traction Control**

  This technology is used mainly for vehicle longitudinal acceleration control. Traction control (TC) distributes driving torque between front and rear axles and drives its restriction. System works on dependence of longitudinal traction force on tire slip ratio λ (Figure 2.3). Thus, traction control prevents from undesirable tire longitudinal slip. It occurs when $\lambda > \lambda_{max}$.

- **Anti-lock Braking System**

  Anti-lock braking system (ABS) purpose is the same as in the traction control case. But it is used at vehicle slow down moment. So it works with braking torques. Again it prevents from undesirable tire longitudinal slip, however in negative part of graph (2.3).

More information about vehicle control systems can be seen in [6].

Chapter 2

Vehicle Modeling

Vehicle model is adopted and modified in this chapter. Tire modeling is described at first. Then triple-track vehicle model is derived.

2.1 Tire Modeling

Tire is the only contact point of vehicle and road surface. All forces for vehicle direction or speed changes are transferred by tires. Therefore its modeling is highly important. Tire vector bases can be seen on Figure 2.1.

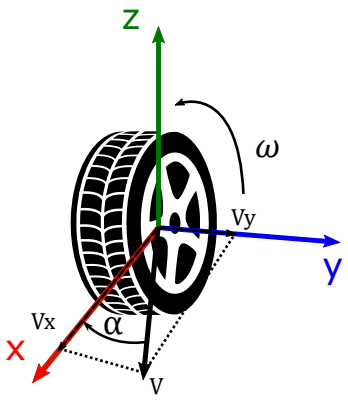

Figure 2.1: Tire coordinate system and tire slip angle α. Angle α orientation is from direction of tire velocity v to axis x and it has positive increment from x axis to y axis.

The tire is oriented in x axis direction, but its direction of motion is given by angle α named tire slip angle:

$$\alpha = -\arctan(\frac{v_y}{v_x}). \tag{2.1}$$

Another important parameter is slip ratio λ giving tire slip amount in longitudinal direction:

$$\lambda = \frac{\omega R - v_x}{\max(\omega R, \mid v_x \mid)}, \tag{2.2}$$

where ω is tire angular speed and R its radius.

Various tire modeling technique are described for example in [5], we are going to approach one of these technique.

2.1.1 Pacejka Magic Formula

Well known and often used formula for lateral and longitudinal forces acting on tires calculation is Pacejka magic formula [10]. This formula was designed by empirical methods by Hans Christian Pacejka so that it would match the tire behavior. Its basis are shaping coefficients – more than 20 coefficients. But there is also the simplified formula with less coefficients. In this thesis formula containing 4 coefficients will be utilised (B, C, D, E) and it is possible to use it for lateral and longitudinal forces and moment of force M_z along z axis calculation:

$$F_y(\alpha) = \mu D_y F_z \sin(C_y \arctan(B_y\alpha - E_y(B_y\alpha - \arctan(B_y\alpha)))) \tag{2.3}$$

$$F_x(\lambda) = \mu D_x F_z \sin(C_x \arctan(B_x\lambda - E_x(B_x\lambda - \arctan(B_x\lambda)))), \tag{2.4}$$

where F_z is tire load and μ is road friction coefficient. If the load increases, tire can generate larger amount of lateral and longitudinal forces. But the peaks take place for same λ a α, and its given by shaping coefficients. There are shown values development of these forces for student formula tires on Figure 2.2 and 2.3

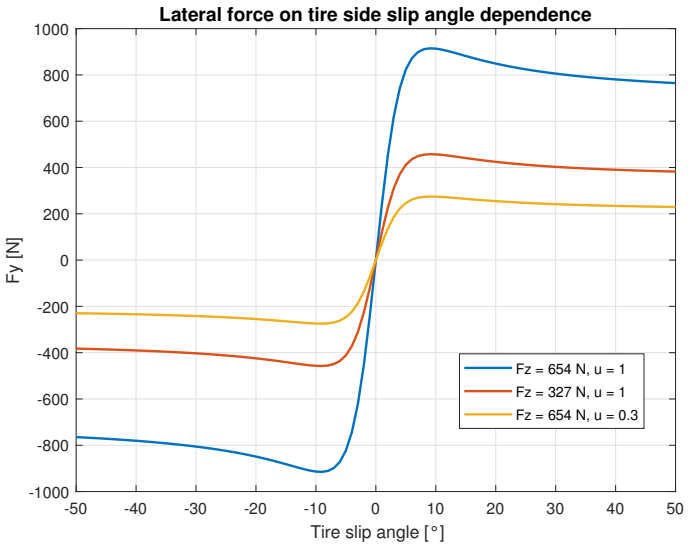

.

Figure 2.2: Quantity of lateral force dependence on tire slip angle is varied with different load and different road friction coefficient. Presented tire parameters are stated in attachment, see Table B.2

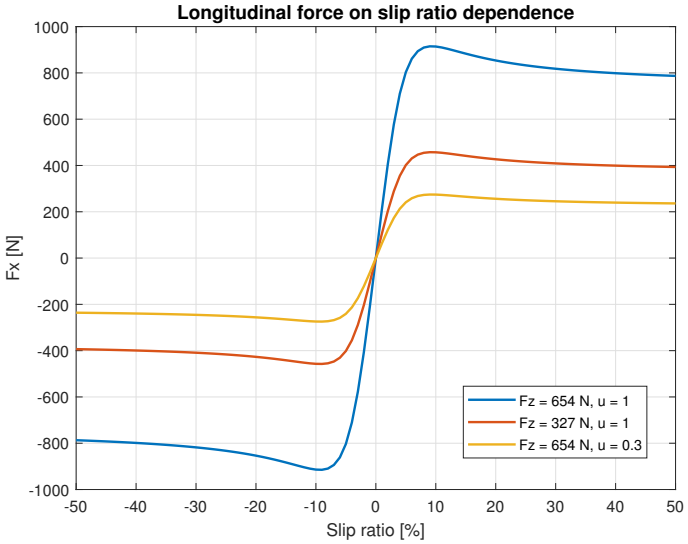

.

Figure 2.3: Quantity of longitudinal force dependence on tire slip angle is varied with different load and different road friction coefficient. Presented tire parameters are stated in attachment, see Table B.2

Maximum (minimum) lateral force for formula tire occurs when $\alpha = 9°$ $(-9°)$, longitudinal force for value $\lambda = 9.3\%$ (-9.3%).

Lateral force F_y actually don't act just in the middle of tire. The distance between lateral force origin and middle of tire is called pneumatic trail. It can be seen on Figure 2.4. That is the reason for self-aligning moment M_z emergence.

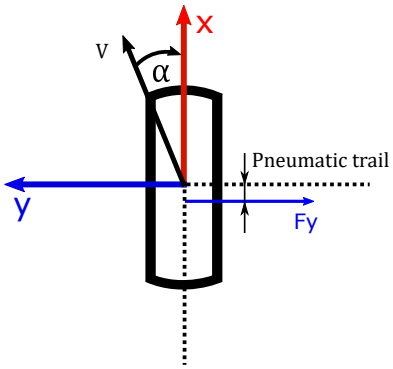

Figure 2.4: Self aligning moment emergence. The reason is lateral force origin and distance named pneumatic trail.

$$M_z(\alpha) = \mu D_z F_z \sin(C_z \arctan(B_z\alpha - E_z(B_z\alpha - \arctan(B_z\alpha)))) \qquad (2.5)$$

But pneumatic trail will be neglected in this thesis and self-aligning moment will be used only for steering wheel feedback in the simulation environment.

2.1.2 Kamm's Circle

The tire is not able to generate arbitrary forces F_x a F_y. These forces are bounded. This restriction is often called Kamm's circle (sometimes called friction ellipse, Figure 2.5). It is relevant if vehicle is within cornering manoeuvre at the same time with acceleration or deceleration. The algorithm for calculation of this limitation was adopted from [2].

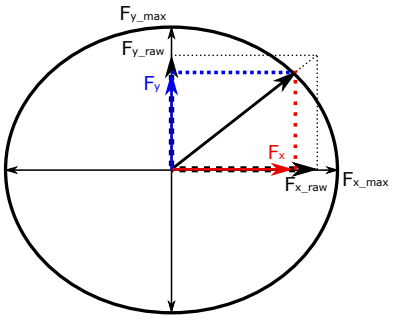

Figure 2.5: Kamm's circle.

2.2 Nonlinear Vehicle Model

Triple-track vehicle model is derived in this section. Triple-track model was derived by single-track model modification to two rear wheels. Single-track model has considerably less states than twin-track models. Instead of 16 states for twin-track [11], only 5 states for single-track [1] and 6-states for (derived below) triple-track. The following model handling, linearization and control design is easier. Despite the states reduction triple-track model will provide enough precision for our purposes model.

This model was with modification adopted from [1]. Vehicle modeling techniques are described extensively in [3], [8] and [11].

Front tires are represented as a single one. Other simplification is that we neglect lifting, rolling and pitching motion. In automotive industry (SAE) is used coordinate system shows on Figure 2.6. Axis x goes from car's centre of gravity (CoG) towards centre of front axle, axis y from CoG towards left side of vehicle and axis z, according to right-handed orientation, from CoG upwards.

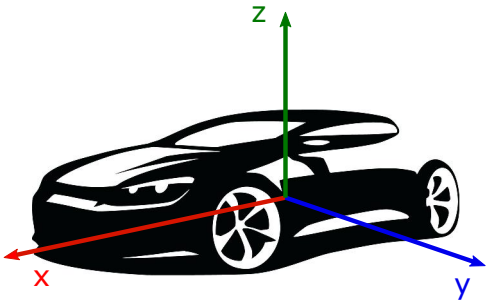

Figure 2.6: Vehicle coordinate system.

The triple-track model is displayed on Figure 2.7, on which v is vehicle velocity, β side slip angle of vehicle defined as $\arctan(v_y/v_x)$, $\dot{\psi}$ represents yaw rate motion (vehicle angular speed around the z axis). Steering angle δ_f is angle between vehicle x axis and front wheel x axis. Only front wheel is steered. Angles orientation is positive along right-handed orientation (Figure 2.6). So angle β on the figure is negative.

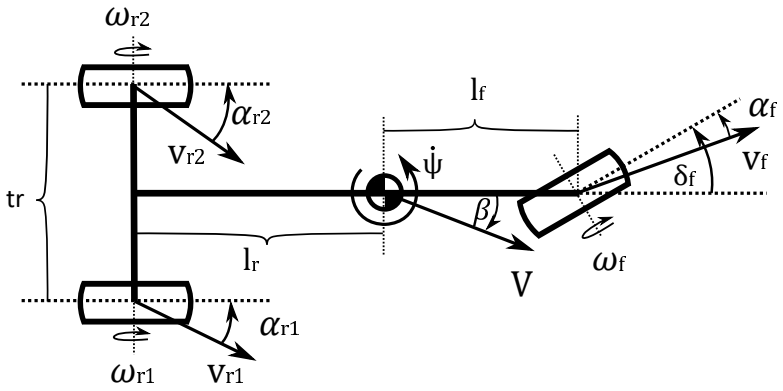

Figure 2.7: The triple-track vehicle model.

On the figure v_f (v_{ri}) there are velocities of front (rear) tire(s). Their velocities directions are defined by front (rear) tire(s) slip angle α_f (α_{ri}). It is needed to determine these angles for tire forces calculation. It is possible to make it by vehicle velocity (quantity and direction) projection to all the wheels. We also take into account vehicle $\dot{\psi}$. For front wheel velocities we can write:

$$v_{xf} = v\cos(\beta - \delta_f) + l_f R\sin(\delta_f) = (v\sin(\beta) + l_f R)\sin(\delta_f) + v\cos(\beta)\cos(\delta_f) \tag{2.6}$$

$$v_{yf} = v\sin(\beta - \delta_f) + l_f R\cos(\delta_f) = (v\sin(\beta) + l_f R)\cos(\delta_f) - v\cos(\beta)\sin(\delta_f) \tag{2.7}$$

For rear wheels applies:

$$v_{xr1} = v\cos(\beta) + R\frac{tr}{2} \tag{2.8}$$

$$v_{xr2} = v\cos(\beta) - R\frac{tr}{2} \tag{2.9}$$

In next equations i is subscript of the right (1) a left (2) rear wheel.

$$v_{yri} = v\sin(\beta) - Rl_r \tag{2.10}$$

Tires slip angles, with regard to definition of positive, angles are:

$$\alpha_f = -\arctan(\frac{v_{yf}}{v_{xf}}) \tag{2.11}$$

$$\alpha_{ri} = -\arctan(\frac{v_{yri}}{v_{xri}}) \tag{2.12}$$

Slip ratio of tires can be obtained if we now substitute Eq. 2.6, 2.8, 2.9 into Eq. 2.4. Now, longitudinal and lateral forces can be acquired (as described in section 2.1.1) 2.8

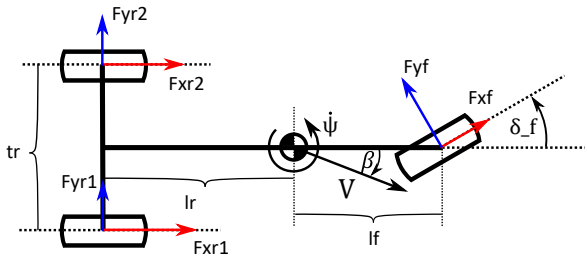

Figure 2.8: Forces generated by tires acting on the vehicle.

On the vehicle (formula) act also longitudinal drag force and vertical pressure force (adopted from [7]):

$$F_{x\_aero} = \frac{1}{2}\rho A C_D v^2 \tag{2.13}$$

$$F_{zf\_aero} = \frac{1}{2}\rho A C_L v^2 (1 - CoP) \tag{2.14}$$

$$F_{zr\_aero} = \frac{1}{2}\rho A C_L v^2 (CoP), \tag{2.15}$$

where ρ is denoted to air density, A is aerodynamic reference area, C_D and C_L are lift and drag coefficient of vehicle body related to the center of pressure (CoP).

Longitudinal F_x (along x axis) and lateral F_y (along y axis) forces and moment of force M_z around z axis acting on the vehicle are:

$$F_x = \cos(\delta_f)F_{xf} - \sin(\delta_f)F_{yf} + F_{xr1} + F_{xr2} + F_{x\_aero} \tag{2.16}$$

$$F_y = \sin(\delta_f)F_{xf} + \cos(\delta_f)F_{yf} + F_{yr1} + F_{yr2} \tag{2.17}$$

$$M_z = l_f \sin(\delta_f)F_{xf} + l_f \cos(\delta_f)F_{yf} + F_{xr1}\frac{tr}{2} - F_{xr2}\frac{tr}{2} - F_{yr1}l_r - F_{yr2}l_r \tag{2.18}$$

The vehicle motion is given by equations:

$$-mv(\dot{\beta} + \dot{\psi})\sin(\beta) + m\dot{v}\cos(\beta) = F_x \tag{2.19}$$

$$mv(\dot{\beta} + \dot{\psi})\cos(\beta) + m\dot{v}\sin(\beta) = F_y \tag{2.20}$$

$$I_z\ddot{\psi} = M_z \tag{2.21}$$

Members $mv(\dot{\beta} + \dot{\psi})$ in Eq. 2.19, 2.20 are given by centripetal forces in curvature motion. I_z is moment of inertia of vehicle around z axis.

From these equations we can get (by multiplying equations sin and cos and their sum):

$$\begin{pmatrix} mv(\dot{\beta}+\dot{\psi}) \\ m\dot{v} \\ I_z\ddot{\psi} \end{pmatrix} = \begin{pmatrix} -\sin\beta & \cos\beta & 0 \\ \cos\beta & \sin\beta & 0 \\ 0 & 0 & 1 \end{pmatrix} \begin{pmatrix} F_x \\ F_y \\ M_z \end{pmatrix}. \tag{2.22}$$

Explicit state space representation:

$$\dot{v} = \frac{1}{m}(\sin\beta F_y + \cos\beta F_x), \tag{2.23}$$

$$\dot{\beta} = -\dot{\psi} + \frac{1}{mv}(\cos\beta F_y - \sin\beta F_x), \tag{2.24}$$

$$\ddot{\psi} = \frac{1}{Iz} M_z. \tag{2.25}$$

2.3 Wheel Model

There are no drive torques or braking torques applied in the model yet. It will be added by next equations adopted from [2], which introduces other state space variables-wheels angular speeds.

$$\dot{\omega}_f = \frac{1}{J_f}(\tau_f - F_{xf}R - sign(\omega_f)\tau_{bf} - k_f v_{xf}) \tag{2.26}$$

$$\dot{\omega}_{ri} = \frac{1}{J_r}(\tau_{ri} - F_{xri}R - sign(\omega_{ri})\tau_{bri} - k_{ri} v_{xri}) \tag{2.27}$$

J is wheel moment of inertia, τ drive torque, τ_b braking torque, F_x is force compute via Pacejka magic formula, R wheel radius. Member kv_x model drag moment, k is a coefficient of this drag.

It was obtained vehicle model given by system with 6 state space variable $v, \beta, \dot{\psi}, \omega_f, \omega_{r1}, \omega_{r2}$ and six inputs $\delta_f, \tau_f, \tau_{r1}, \tau_{r2}, \tau_{bf}, \tau_{br}$.

2.4 Linear Model

It is necessary to derive linear vehicle model for further purpose of creating controllers and varied analyses. This linear model will be valid in small

deviation from operating point, in which it was obtained. As the system has 6 states and 6 inputs it results in many operating points. For this reason operating points were chosen in steady states of system ($\dot{v} = 0, \dot{\beta} = 0, \ddot{\psi} = 0, \dot{\omega}_f = 0, \dot{\omega}_{r1} = 0, \dot{\omega}_{r2} = 0$) for various velocities and yaw rate values. Input values and remaining states values, which keep system in steady state, were gained via trimming tool made by David Vošahlík. This tool finds these values by minimization function ($w_1 \cdot \dot{v} + \ldots + w_6 \cdot \dot{\omega}_{r2}$), where w_i are weights. All of this is based on MATLAB optimization function *fmincon*.

Acquired linear model for triple-track model with different drive torques on rear axle has following form (deviation model):

$$\begin{pmatrix} \dot{v} \\ \dot{\beta} \\ \ddot{\psi} \\ \dot{\omega}_f \\ \dot{\omega}_{r1} \\ \dot{\omega}_{r2} \end{pmatrix} = A \begin{pmatrix} v \\ \beta \\ \dot{\psi} \\ \omega_f \\ \omega_{r1} \\ \omega_{r2} \end{pmatrix} B \begin{pmatrix} \delta_f \\ \tau_f \\ \tau_{r1} \\ \tau_{r2} \\ \tau_{bf} \\ \tau_{br} \end{pmatrix} \tag{2.28}$$

2.5 Model Validation

Model derived above had to be validated for further purposes of control. Now data measured during formula drive were compared with data from model obtained with same inputs.

Figure 2.9 shows output variables $\dot{\psi}$ and β of formula and model for the same inputs.

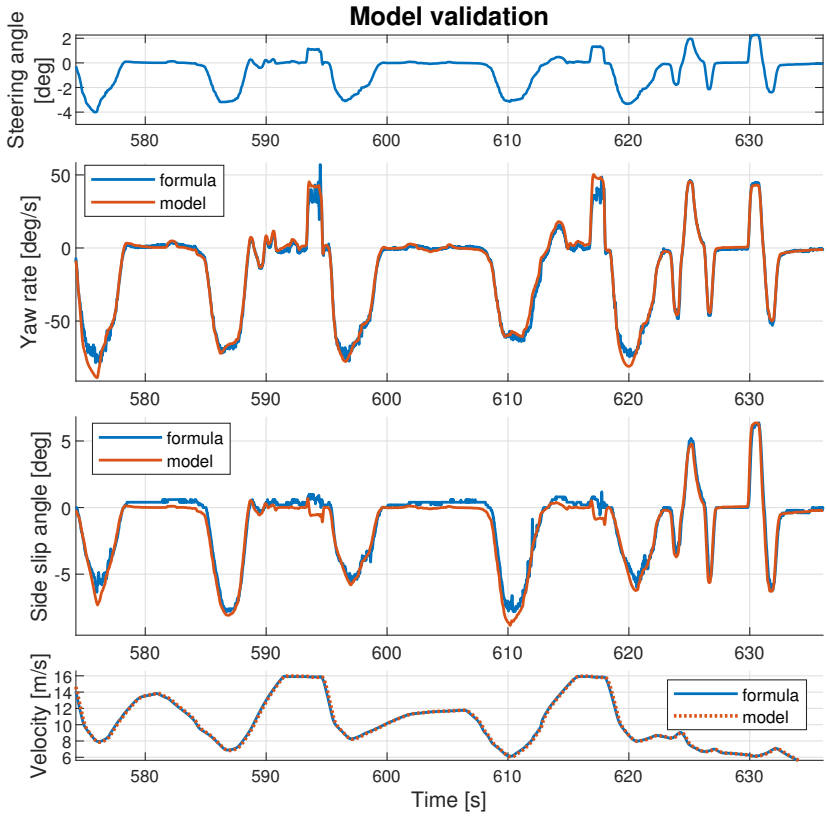

Figure 2.9: Model yaw rate and side slip angle validation.

It should be validated and compared formula and model slip ratios here. But it is not. The reason is faulty slip ratio measurement in formula and noise, which this measurement causes. More in Chapter 6 and Figure 6.2.

Chapter 3

Vehicle Analysis

3.1 Understeering, Oversteering and Neutral Vehicle

It is necessary to understand vehicle stability/instability for purpose of changing its dynamics. Stability is also related with labels understeering, oversteering and neutral vehicle. Understeering vehicle steer less than amount of steering angle given by the driver, its opposite is oversteering vehicle. According to amount of given steering angle steer neutral vehicle. Figure 3.1 shows comparison of these vehicles within cornering manoeuvre.

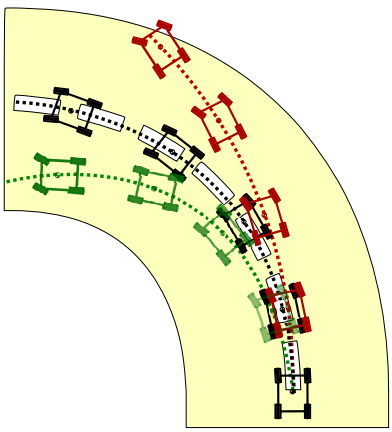

Figure 3.1: Comparison oversteering (green), neutral (black) and understeering (red) vehicle in cornering manoeuvre.

Exact definition of these concepts will be introduced according to [1]. It uses so-called understeering gradient K. Understeering gradient K is defined as:

$$K = (\frac{l_r}{C_f} - \frac{l_f}{C_r})\frac{m}{2(l_f + l_r)}, \tag{3.1}$$

where C_f and C_r are cornering stiffness coefficient of the front and rear tires. According to sign of K we distinguish:

- $K > 0$, understeering vehicle,
- $K = 0$, neutral vehicle,
- $K < 0$, oversteering vehicle.

The sign of K is given only by expression $(l_r/C_f - l_f/C_r)$. It means:

- $l_r C_r > l_f C_f$, understeering vehicle,
- $l_r C_r = l_f C_f$, neutral vehicle ,
- $l_r C_r < l_f C_f$, oversteering vehicle.

With regard to the front and rear tires of formula are the same, it depends only on position of centre of gravity. It is located closer to front axle (see formula parameters in Table B.1), so formula is understeering vehicle.

Further according to [1]:

- Vehicle is stable, if it's understeering or neutral steering.
- Vehicle is unstable, if it's oversteering, from certain critical speed.

Thus, neutral vehicle steer according to steering angle demand by driver and it's stable for all velocities.

3.2 Vehicle Motion Behavior Analysis

Vehicle behavior was analyzed for various speeds from 4 m/s and various cornering manoeuvres. An effect of difference torques at rear axle on run yaw rate and side slip angle was investigated closely. At first linear models for different operating points and transfer functions from torques to $\dot{\psi}$ and β were studied. Then verification on non-linear model was performed.

Now different torques on rear axle wasn't considered. Variable $\dot{\psi}$ value development for various steering angle δ_f in different speeds is expectable. If the car is not in critical situation (skid, spin) then greater steering angle mean greater $\dot{\psi}$. An interesting fact occurs for β values development. Under certain speed β and δ_f have the same sign and greater δ_f means greater steady value β. Run changes after reaching this speed and sign δ_f a β are opposite in stable states. The vehicle velocity direction points to the opposite side then wheels. This speed was found out by experiment in simulation environment, but also from step responses for various speeds. And its value is approximately 14.5 m/s for formula (Figure 3.2).

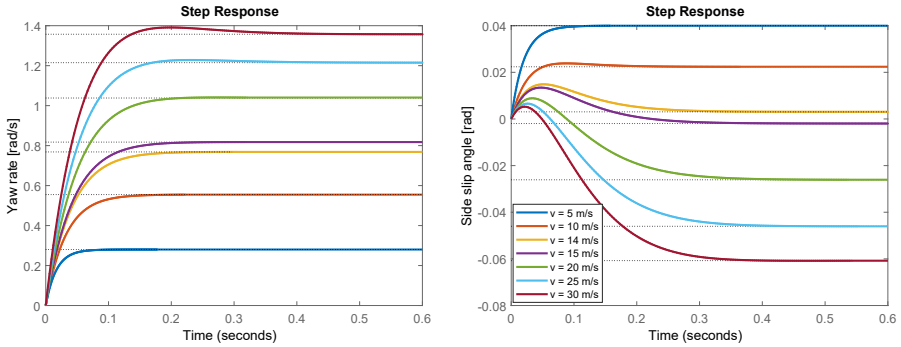

Figure 3.2: Yaw rate and side slip angle response on steering angle δ_f step for different speeds.

However analysis regarding different drive torques on rear axle is more important because of further control design. It was found out, by transfer function analysis and verification on non-linear model, that positive difference $\tau_{r1} - \tau_{r2}$ creates positive increase of $\dot{\psi}$. Conversely this positive difference creates negative increment β for all speeds and angles δ_f. The course change β that was found out for certain speed don't affect the transfer function $\tau_{r1} - \tau_{r2}$ on β. On Figure 3.3 can be seen comparison of course of these quantities for various speeds.

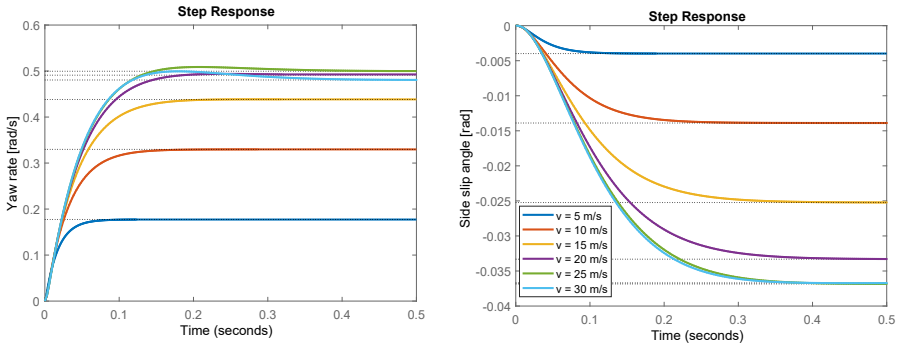

Figure 3.3: Yaw rate and side slip angle response on difference rear torques $\tau_{r1} - \tau_{r2}$ step for different speeds.

3.3 Vehicle Dynamics with Torque Vectoring

Torque vectoring, causing different drive torques on wheels on rear axle, creates additional yaw moment, which affects the vehicle dynamics. Torque vectoring should not change overall torque on rear axle required from a driver (for example produced by traction control). This can be achieved only by symmetrical distribution of additional drive torque:

$$\tau_{r1} = \frac{\tau_r}{2} + \Delta\tau \tag{3.2}$$

$$\tau_{r2} = \frac{\tau_r}{2} - \Delta\tau, \tag{3.3}$$

where τ_r is from driver required torque on rear axle and $\Delta\tau$ is the half of difference between right and left rear wheel. Additional moment ΔM_z around the z axis can be computed as:

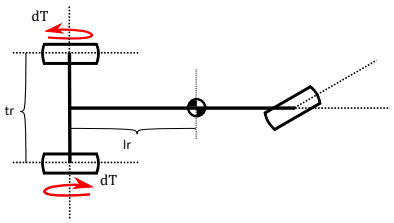

Figure 3.4: Different torques on wheels on rear axle changes vehicle yaw moment. But it changes also another lateral and longitudinal vehicle behavior.

$$\Delta M_z = \frac{\Delta\tau}{R}\frac{tr}{2} + \frac{\Delta\tau}{R}\frac{tr}{2} \tag{3.4}$$

Addition of additional moment as it was done above in Eq. 3.4 is a bit inaccurate and is incorrect. (As above it was also done in [9] and [7], because in these theses longitudinal dynamics was neglected.) Actually, torques from Eq. 3.2, 3.3 are inputs in Eq. 2.27 and real additional moment acting on the vehicle is calculated by forces obtained from Pacejka Magic formula. Just to calculate right this torques difference on rear axle it was necessary create vehicle model with two rear wheels. In single-track model is this impossible.

From the model derivation it is clear that this torques difference don't affect only vehicle yaw moment around z axis, but also longitudinal and lateral (by Kamm's circle) force acting on the vehicle. So it changes overall vehicle dynamics. The impact on slip ratios of both rear wheels is essential. Again we can make request leads to Eq. 3.2, 3.3. But we don't have to strictly insist on this requirement, because it don't express what we actually want. This demand should be defined rather following way:

$$F_{xr1} = \frac{F_{xr}}{2} + \Delta F_{xr} \tag{3.5}$$

$$F_{xr2} = \frac{F_{xr}}{2} - \Delta F_{xr}, \tag{3.6}$$

where F_{xr} is longitudinal force on rear axle and ΔF_{xr} half of difference of longitudinal forces between right and left rear wheel. The lack of this information about force F_{xr} is a problem(if we know road friction coefficient μ and slip ratio λ_{ri} we only can calculate F_{xr1} a F_{xr2}). Overall drive torque on rear axle don't determine the force which should rear axle generate. This happens after specific distribution of this torque to right and left wheel (and considering its states).

This problematics of drive torque distribution while maintaining tractive force is discussed in section 4.2.

Chapter 4

Proposed Control Algorithms

Common goal of all proposed algorithms will be vehicle's lateral behavior change, so it would be identical with neutral vehicle dynamics. Thus, neutral vehicle based on model created in 2 would be reference vehicle for us.

Modification of lateral dynamics means modification of formula angular speed around centre of gravity $\dot{\psi}$ and change side slip angle β of formula. If only one of these quantities would be changed according to the reference vehicle, it wouldn't be recognized, whether the other one is wasn't considerably deviated from the same quantity of neutral vehicle. And so whether vehicle didn't perform complete different motion. On Figure 4.1 are these cases stated.

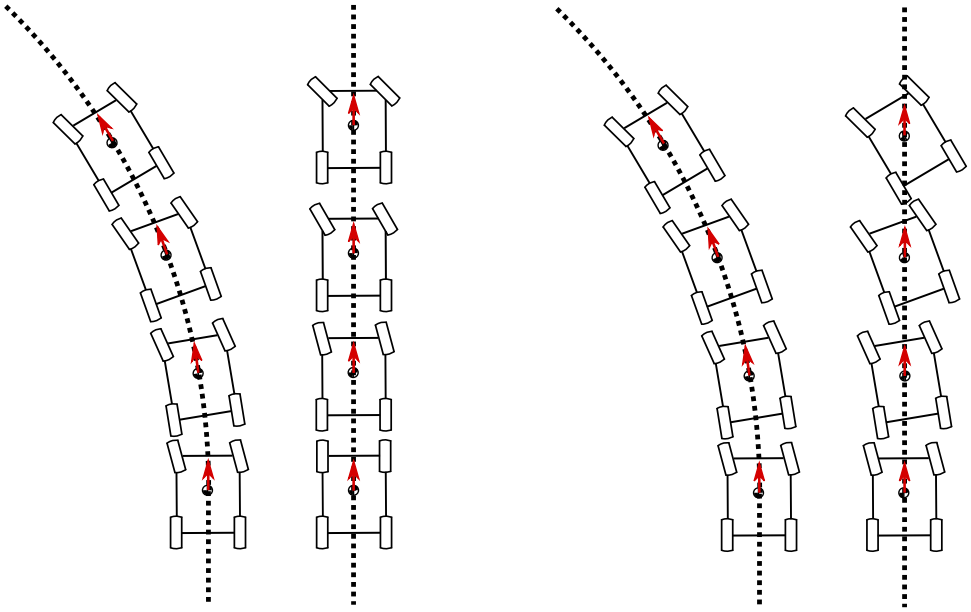

Figure 4.1: Two vehicles on left side of the figure perform different motion, however their β is identical. Same value of quantity $\dot{\psi}$ have two vehicles on the right side of figure, but their motion is also different. That's the reason why would both of these quantities represent references for proposed algorithm. Red arrows label vehicle's direction.

In proposed control algorithms we would try to modify both of these quantities according to reference vehicle. Both of these quantities would represent references. Compromise between these quantities would be necessary for purpose of control.

Torques distribution between front and rear axle is resolved by traction control. The output is torques τ_f a τ_r. Control variable will be changed of torques on rear axle according to torque vectoring functionality. On front axle torques won't be changed. This is displayed in schematic on Figure 4.2.

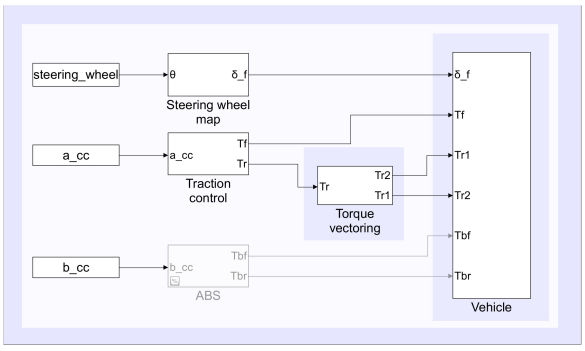

Figure 4.2: Overall approach to vehicle control.

4.1 Yaw Rate and Side Slip Angle Control

First proposed control algorithm for torque vectoring functionality can be seen on Figure 4.3

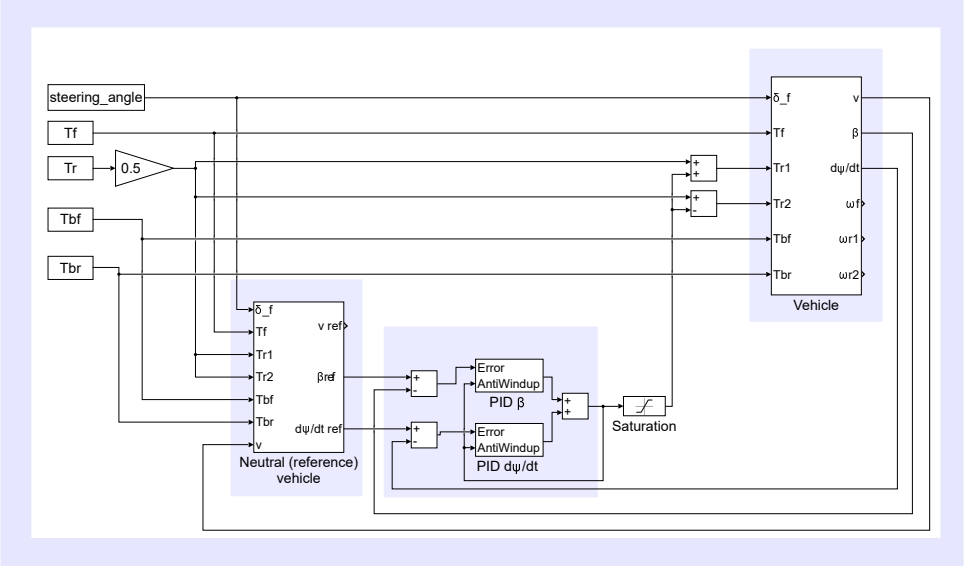

Figure 4.3: Control algorithm for torque vectoring functionality. Controllers PID β and PID $\dot{\psi}$ create torque, which is distributed symmetrical between right and left rear wheel.

At first, controller $\dot{\psi}$ was designed, so it minimized the error and it created stable system. Thus, controller $\dot{\psi}$ could works independently without β controller. Then controller β for overall new created system was designed. Saturation limits drive torques. They should be smaller than minimal and greater than maximal possible for given motors. It's used clamping antiwindup system.

Reference vehicle velocity have to be the same as velocity of steered vehicle, otherwise reference values wouldn't be valid. Therefore input to this system is also velocity. Inside of neutral vehicle model is computed additional longitudinal force by controller. But these values are small and affect on longitudinal dynamics is low.

It's clear that it's not possible to control both process variable $\dot{\psi}$ and β precisely by single control variable $\Delta\tau$. Hence controllers were designed for their almost same power, but controller $\dot{\psi}$ was designed slightly powerful. And it tracks the reference more accurately. Later the reason will be shown.

From this reason (one control variable, two process variable) Linear – Quadratic – Integral control (LQI) was designed. LQI is advanced part of control by state feedback with an integral control. It introduces weighting matrices, which user proposes based on requirements form the system. Based on the matrices algorithm minimize certain cost function. By designing weighting matrices it is possible to give weights to individual signals (thus also $\dot{\psi}$ and β). In this case we have two output variables, which we want to control, LQI will consist of two integrators as well.

Unfortunately results of this algorithm (LQI) were not better than results above given algorithm, and that is the reason why we continue our work only with first algorithm 4.3.

4.2 Slip Ratio Control System for Torque Vectoring Functionality

This section extends algorithms for torque vectoring functionality developed in section 4.1 about slip ratio control system. Next calculated situations are motivation for this extension:

- A vehicle accelerates considerably and slip ratio of both wheels on rear axle approaches λ_{max}. Additional change of torque by torque generates from TV would cause undesirable tire slip on one of the tires.
- One of the rear wheels starts slip significantly in contrast to the other one. (For example because it moves on different surface (ice)). Situation can be improved by decreasing the drive torque on this one wheel, but mainly also on the other one.
- Torque vectoring creates big difference between torques on rear axle. One of the wheel approaches λ_{max}, the other one λ_{min}. This case in relevant only on surface with low friction coefficient μ.

These situations can be solved by slip ratio control for torque vectoring (TV SC).

Below introduced algorithm (Figure 4.4) for slip ratio control is based on following reason. TV creates different torques on rear wheels. These torques spin wheels and makes different slip ratio on these tires. Slip ratios according

to Eq. 2.4 generate longitudinal forces. Created difference between these forces affects vehicle dynamics. By using superior controllers for $\dot{\psi}$ and β a reference can be generated for the difference of $\lambda_{r1} - \lambda_{r2}$. By adding a half of this difference to the slip ratio value of a neutral vehicle on the right tire given by demand on τ_r created in traction control we obtain a reference for λ_{r1}. By subtracting half of this difference from the slip ratio value of a neutral vehicle on the left tire given by demand on τ_r created in traction control we obtain a reference for λ_{r2}. Desired torques on wheels can be calculated from errors λ_{r1} and λ_{r2} by using regulators in inner loop. This algorithm can completely control and limit slip ratios on both wheels. Concurrently, algorithm respects torques created in traction control because it works with neutral vehicle slip ratios.

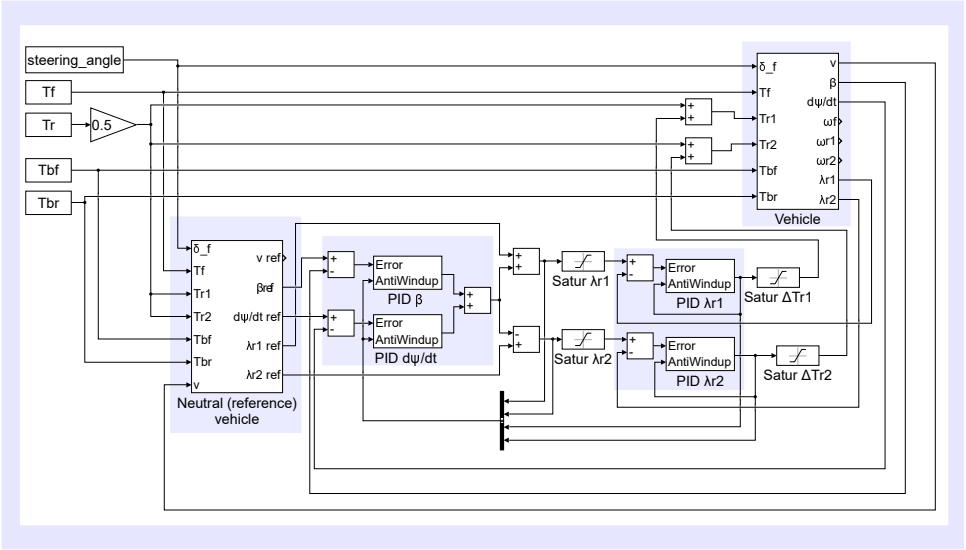

Figure 4.4: Proposed control algorithm for torque vectoring functionality based on the slip ratio control.

It's possible to choose from several methods to modify saturation limits and control variables $\Delta\tau_{r1}$ and $\Delta\tau_{r2}$, for example (subscript raw means $before\ saturation$):

- Select $\Delta\tau_r = \min(|\ \Delta\tau_{r1\_raw}\ |, |\ \Delta\tau_{r2\_raw}\ |)$, then

$$\Delta\tau_{r1} = sign(\Delta\tau_{r1\_raw}) \cdot \Delta\tau_r,$$

$$\Delta\tau_{r2} = sign(\Delta\tau_{r2\_raw}) \cdot \Delta\tau_r.$$

- If $\Delta\tau_{r1\_raw} > 0$ select

$$\Delta\tau_{r1} = \min(|\ \Delta\tau_{r1\_raw}\ |, |\ \Delta\tau_{r2\_raw}\ |, |\ min(\Delta\tau_{r2\_raw}, 0)\ |).$$

If $\Delta\tau_{r2\_raw} > 0$ select

$$\Delta\tau_{r2} = \min(|\ \Delta\tau_{r1\_raw}\ |, |\ \Delta\tau_{r2\_raw}\ |, |\ min(\Delta\tau_{r1\_raw}, 0)\ |).$$

Many methods from which can be chosen from are almost always trade-offs between vehicle stability and acceleration. (Also tractive force or drive torque maintaining is consider). The following method which was chosen prefers stability over acceleration and therefore it can modify (decrease) required torque on rear axle:

Saturation values of slip ratios are given and they are not mutually modified. Also saturation values of torques are given only by motors limits. If one of the branches reaches saturation (one of the saturations λ_{r1}, λ_{r1}, $\Delta\tau_{r1}$, $\Delta\tau_{r2}$) a clamping antiwindup is implemented to turn off integral terms PID β and PID $\dot{\psi}$. If $\Delta\tau_{r1}$ reaches saturation the clamping is used to turn off PID λ_{r1}. Also in case of $\Delta\tau_{r2}$ saturation PID λ_{r2} integral term is turned off.

The main benefit of this method is that both of the desired slip ratios can be tracked. Another advantage occurs when one of the branches (for left or right wheel) is saturated (either based on λ_{max} or torques saturation). It is still possible to use torque on the other wheel for TV better functionality (vehicle stability). However, if the signals are between saturation limits, control variables $\Delta\tau_{r1}$ and $\Delta\tau_{r2}$ are almost identical except for sign.

This algorithm is also effective if the rear wheels travel on a different surface. Consider model situation:

Right wheel gets on slippery road and starts to slip. Thus, the right tire starts to generate smaller force and vehicle turns right. Therefore a deviation from the reference vehicle raises. Controllers PID β and PID $\dot{\psi}$ will generate a positive difference $\Delta\lambda$. Controller PID λ_{r1} will respond to slip change and reference change at the same time and starts modify torque τ_{r1}. Controller PID λ_{r2} will respond to reference change by large reduction of torque τ_{r1}.

It would be very useful to determine current friction coefficient μ of the road. This additional information can be used in reference model. Friction coefficient μ can be calculated from λ of the tire and computation longitudinal force generated for λ by the tire. Unfortunately the system for computing force generated by a single tire is not implemented in formula.

4.3 Steering Angle Control with Torque Vectoring

Both previous presented algorithms do have common attribute, as they don't achieve (and they can't) track both process variable $\dot{\psi}$ and β concurrently. Here, we try to propose control algorithm, which would solve this.

Let's assume that driver don't steer vehicle wheels by steering wheel directly and let's consider steering wheel angle like requirement for vehicle turning amount. Steering angle δ_f would be controlled by algorithm (Figure 4.5). However, intervention to steering should not be large. Algorithm with reference variable $\dot{\psi}_{ref}$ will be proposed. Control variable would be steering angle δ_f. TV functionality we add to this so vehicle can track also β_{ref}. We can completely change lateral vehicle dynamics to neutral.

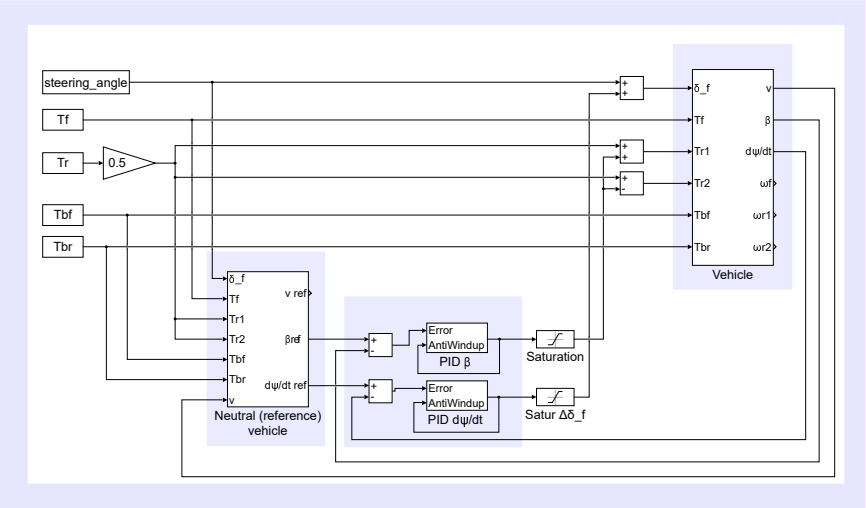

Figure 4.5: Control algorithm based on torque vectoring functionality for β control and $\dot{\psi}$ control by steering angle δ_f.

The reason why is chosen $\dot{\psi}$ control by changing δ_f and β control by TV is obvious from 3.2. By modification δ_f it is easier to control $\dot{\psi}$ than β. (This variable can be well driven by steering rear wheels)

This function isn't feasible on student formula, therefore variables values development will be tested only in simulation environment. It wasn't main aim of this thesis to solve this task. However, it is presented here, because it means possibility how to take over more supervision of vehicle and increase driver's comfort in the future. For example, it happens a lot in crises situation that driver, who wants to solve this critical situation, steers the steering wheel

too much. It causes increasing tire slip angle, which can exceed α_{max}, and then the force which is tire able to transfer decreases (Eq. 2.3 and Figure 2.2). This way of vehicle steering, when driver don't control chassis directly but gives requirement for steering which algorithm evaluates, could also prevent from this situation.

The main torque vectoring disadvantage is lower limitation on drive torques. If a driver don't use the gas pedal and drive torque on rear wheels is zero, TV is hardly useful, particularly in cases (vehicles) which don't allow non negative torques. (On formula this demand isn't that strict, but it should not happen that both torques will be negative at the same time.) The same restriction represent also upper limit. Nevertheless, in cornering manoeuvre the first case is more frequent. Torque vectoring (TV) and steering angle control with torque vectoring (TV+SAC) comparison is shown in Chapter 5.

4.4 Reference Model States Actualization

In case of an oversteering vehicle (unstable) TV helps stabilize the vehicle. If a driver steers, a vehicle with TV should steer less than a vehicle without TV (ideally as a reference neutral vehicle). If the oversteering vehicle get to a skid, the reference vehicle may not be in this skid. Different situation occurs in our case of an understeering vehicle. (Formula is the understeering vehicle, see Table B.1). There can also happen the situation when formula with TV will not be able to reach states $\dot{\psi}$ and β of reference vehicle for a certain input configuration (torques and steering angle). That happens for example because of limits for torques, which can be used for TV, or because the tire will be in excessive slip, or because it is not possible track the reference $\dot{\psi}$ and β concurrently. Formula may not get to a skid, although reference vehicle model will be in a skid. States of reference model start deviate from formula states. If the vehicle leaves off cornering manoeuvre, states of reference model can be completely different.

This problem is displayed on next Figure 4.6 from extreme situation simulation.

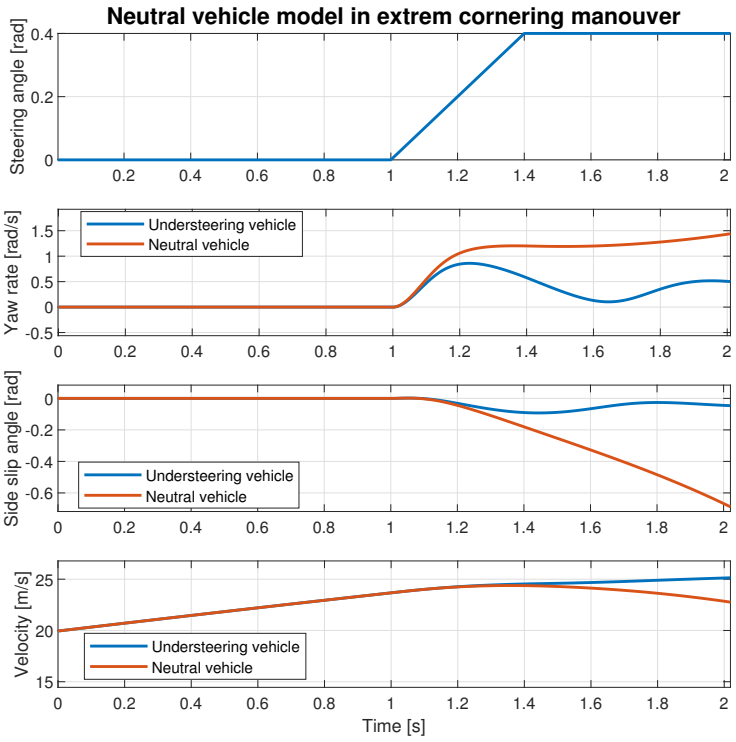

Figure 4.6: Neutral vehicle can get to skid, whereas understeer vehicle can handle this situation for same inputs (steering angle, torques).

Vehicles starts cornering manoeuvre at time 1 s. It can be seen from $\dot{\psi}$ and β course that neutral vehicle turn more than understeering vehicle. Neutral vehicle gets extreme skid after a while. Its states are completely different and vehicle can't be steered by it.

Although these situations don't occur frequently, this problem is important. So it is needed to solve it. Two solutions of these situations will be proposed. Set the states of reference vehicle to current states of steered vehicle, when states of reference vehicle approach certain value, can be the first one. Variable β of formula doesn't approach values over (under) approximately $25°$ ($-25°$) during the drive. Therefore the value (for example) $30°$ can be defined as boundary and values of formula over (under) this boundary consider as undesirable. States of reference vehicle will be set to vehicles states after reaching this boundary.

The other option specifies maximal differences between vehicle and reference vehicle states. In this case the states of reference vehicle artificially keep under these differences.

Both methods do have their weaknesses. The first one creates artificially step changes. Furthermore states can after the resetting (if the driver still perform the same manoeuvre) reaches the boundary again. The other one seems to be better in this way. But again it requires boundary definition at which these maximal differences will be activated. Otherwise it can also happen that in case of situation in no way extreme these differences affect the vehicle dynamics.

Chapter 5

Simulation Tests

5.1 Simulation Environment

Functionality of proposed algorithms was validated in simulation environment. Software IPG Carmaker [4] was chosen for its high fidelity behaviour with real vehicle behaviour. IPG Carmaker allows to set vehicle parameters, so that they match with real vehicle. Then drive ability of both vehicles are comparable and test results in simulations can be considered as matching with reality. More information about software, validation parameter of formula model in IPG Carmaker but also algorithm implementation into formula can be found in Marek László master thesis [7].

5.2 Simulation Results

In this section results and action principles of proposed control algorithms will be pointed out.

Functionality of algorithm 4.3 TV without slip ratio control was tested at first. Variables values course during simulation tests are shown on Figure 5.1.

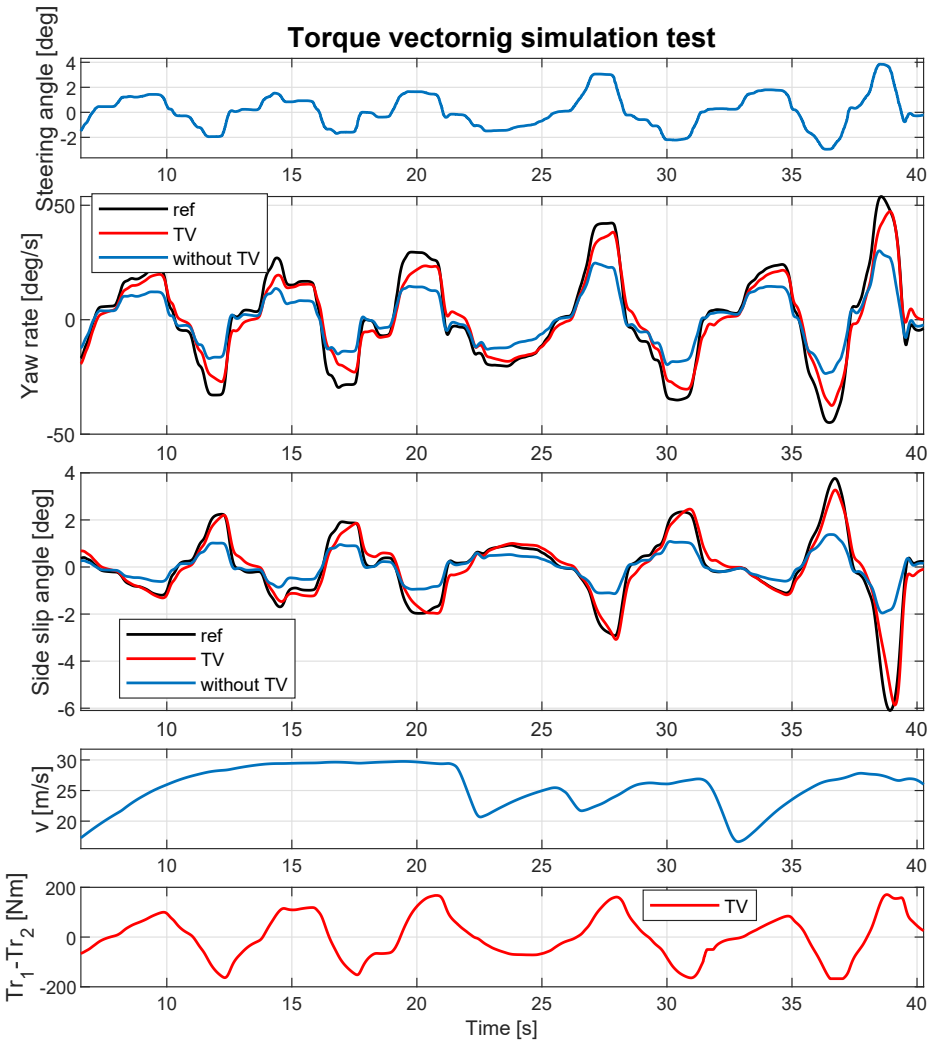

Figure 5.1: Output variables $\dot{\psi}$ and β during the simulation of algorithm TV in IPG Carmaker. Control variable is difference of torques $\tau_{r1} - \tau_{r2}$.

From this figure it is clear that vehicle dynamics was improved. And although vehicle don't exactly track the reference vehicle, its lateral dynamics approaches reference vehicle dynamics. Motors could generate negative drive torque (lower limit was -50 Nm after transmission) in this simulation. Formula allows motors to do this. Thus, TV could work without using gas pedal.

Next proposed algorithm 4.4 TV with slip ratio control (TV SC) was tested for various restrictions of maximal (and minimal) slip ratio value. Upper boundary of these restrictions can be effectively controlled, unfortunately lower boundary is possible to control only if the driver don't use brakes. Torque vectoring control only drive torques and can't affect brake torques.

Data from drive test with restriction $\lambda = \pm 2\%$ are shown on Figure 5.2.

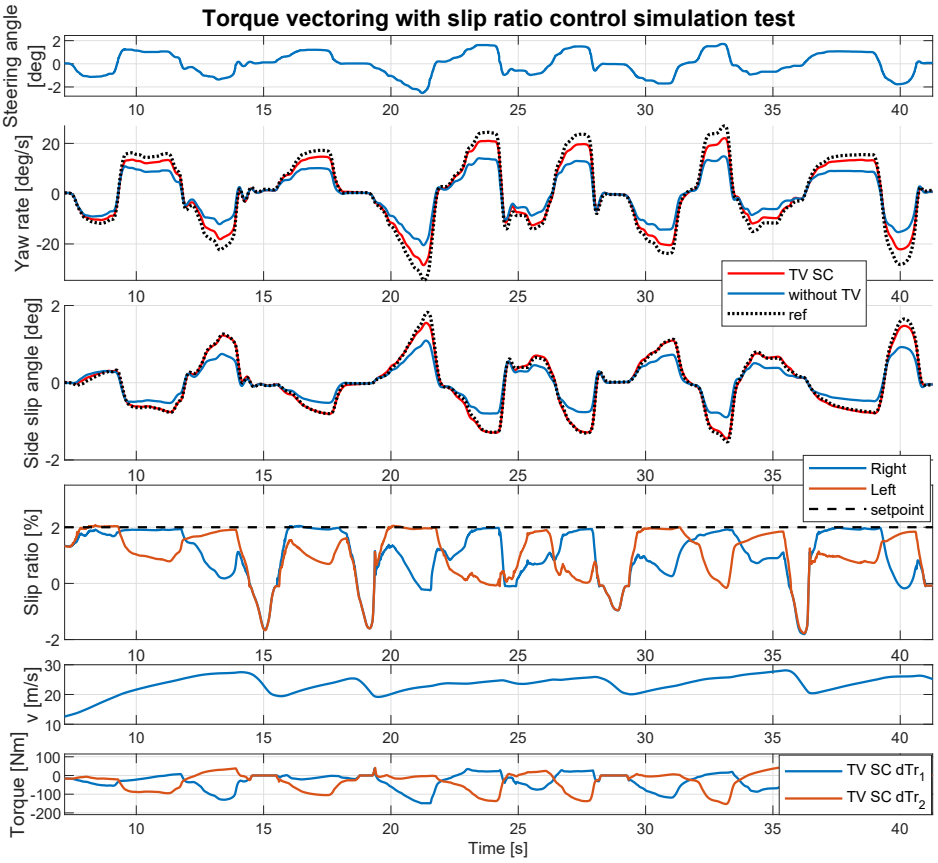

Figure 5.2: Output variables $\dot{\psi}$ and β during the simulation TV SC in IPG Carmaker. Control variables are additional torques $\Delta\tau_{r1}$ and $\Delta\tau_{r2}$. Slip ratio of both tires don't exceed set boundary.

Apparently, the vehicle dynamics was improved, despite low upper slip ratio value boundary. The reason behind is the emphasis put on vehicle stability and its lateral dynamics described in section 4.2. If the slip ratio value of either one of the wheels get to upper boundary of restriction, the other one starts to descend. Also, it is obvious from variables $\Delta\tau_{r1}$ and $\Delta\tau_{r2}$ development, their range is rather in negative part of graph. The vehicle is slowed down.

This trend is also evident from comparison of variables values development for various slip ratio restrictions, which are displayed on next Figure 5.3. Comparison of restrictions $\lambda = \pm 2\%, \pm 3\%, \pm 9.3\%$ is drawn.

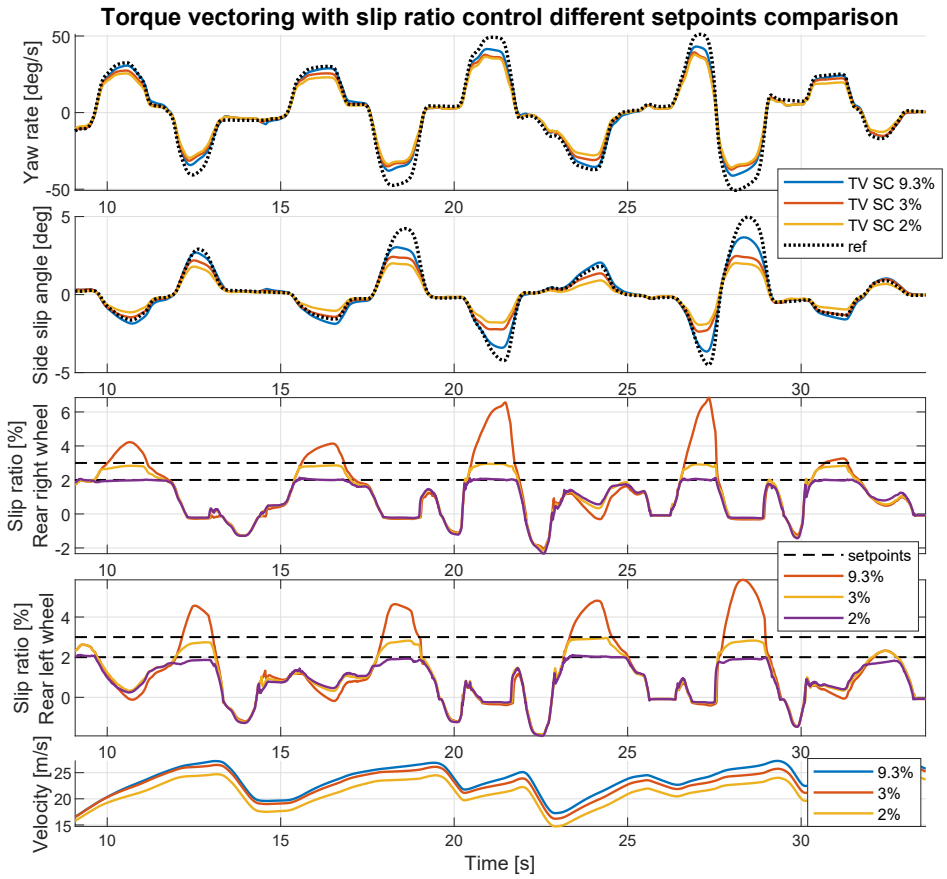

Figure 5.3: Output variables $\dot{\psi}$ and β during simulation TV SC in IPG Carmaker. Comparison for various restrictions λ_{max} is drawn. Slip ratio values of tires don't exceed this boundaries.

It is possible to find out, that algorithm with upper limit $\lambda_{max} = 9.3\%$ do track the output variables better than algorithms with boundaries 3% and 2%. But this difference is not large. Once again the reason behind is control variables $\Delta\tau_{r1}$ and $\Delta\tau_{r2}$. Their magnitude matches λ_{r1} and λ_{r2} on described figure. Velocity of vehicle steered by algorithm TV SC 9.3% is not restricted (because λ don't reach upper limit) and drive torques on rear axle are distributed symmetrically between right and left wheel around required value. Algorithms TV SC 3% and TV SC 2% do slow down the vehicle to achieve better lateral behavior. (Slip ratio average is bigger for TV SC 9.3% than for TV SC 3% (2%).)

Next figure 5.4 compare algorithms TV and TV with slip ratio control on common surface with friction coefficient $\mu = 1$.

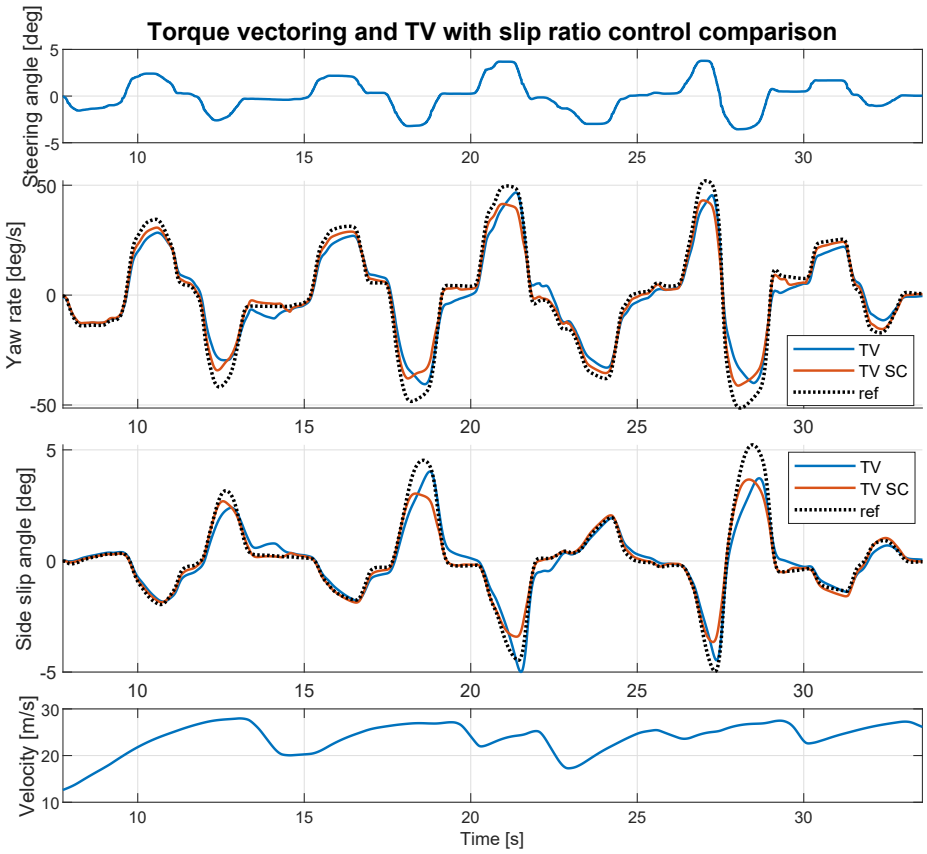

Figure 5.4: Output variables $\dot{\psi}$ and β during the simulation in IPG Carmaker. Comparison algorithms TV and TV SC for friction coefficient $\mu = 1$

Algorithms do have similar performance, although small differences are apparent. TV SC acts faster, TV reaches higher values. But this is given mostly by designed controllers and drive torque limitation (TV was allowed to use negative torque in contrast with TV SC), and not by action principle of these algorithms. But the difference between these two approaches would be evident from further graph. There is comparison of these algorithms for slippery surface with friction coefficient $\mu = 0.7$ on Figure 5.5.

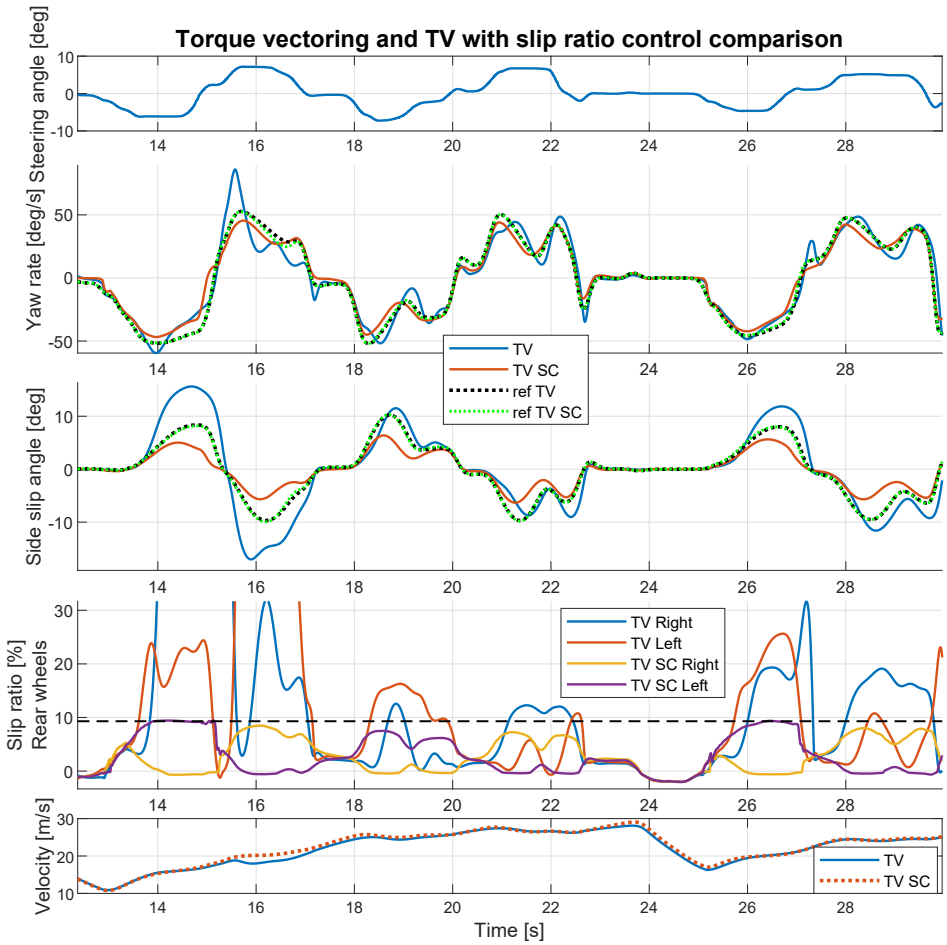

Figure 5.5: Output variables $\dot{\psi}$ and β during the simulation in IPG Carmaker. Comparison of algorithms TV and TV SC for friction coefficient $\mu = 0.7$ is drawn.

It is clear from this figure that vehicle with TV with slip ratio control (TV SC) do achieve better results than vehicle driven by TV without slip ratio control. The reason is just the slip ratio control. Slip ratios of algorithm TV SC don't exceed the restriction $\lambda_{max} = 9.3\%$ and therefore it can track the neutral vehicle without undesirable skid or slip.

The last test from simulation in this section examines possibilities of front wheels steering angle control. There are compared algorithms TV 4.3 and TV with steering angle control (TV+SAC) 4.5 on Figure 5.6.

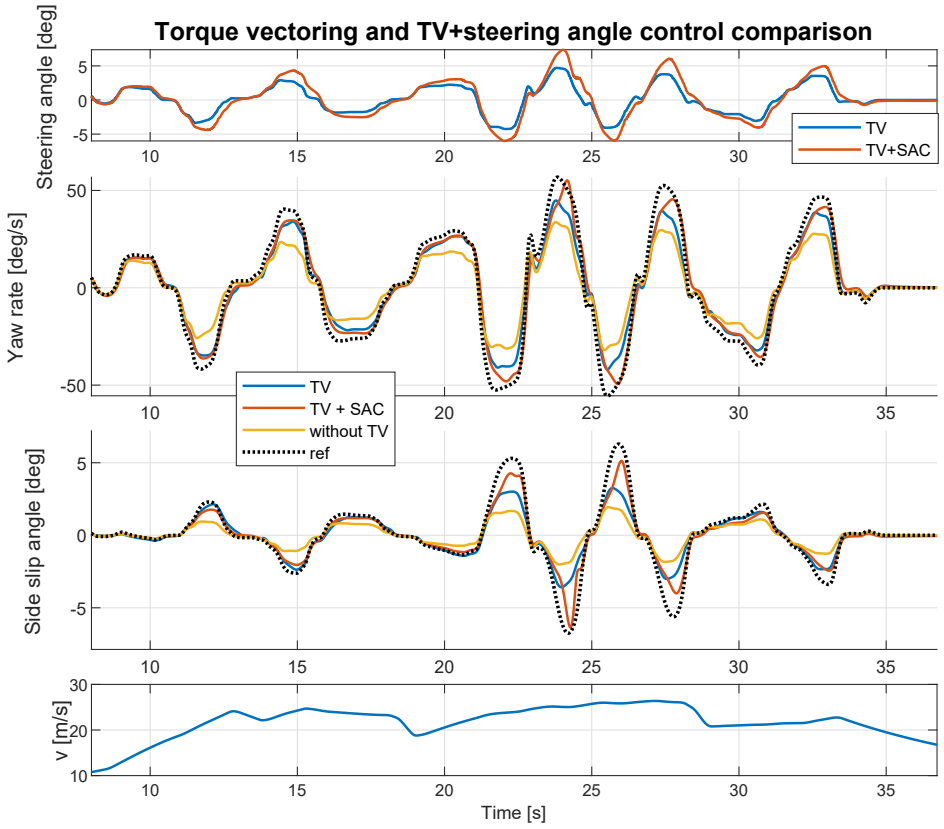

Figure 5.6: Output variables $\dot{\psi}$ and β during the simulation in IPG Carmaker. Comparison algorithms TV and TV with steering angle control is drawn.

From this variables values development we can state that TV+SAC reaches better results than TV (Although designed controllers should be improved, about time 24.5 s small oscillations of steering angle δ_f can be seen). For this measurement torques wasn't allowed to reach negative values. If we have this restriction (and it is in many situations), TV has in case of low required torque to rear axle poor options for modification lateral dynamics. On the other hand steering angle control can cause its improving in this case.

Another advantage will be shown on next Figure 5.7.

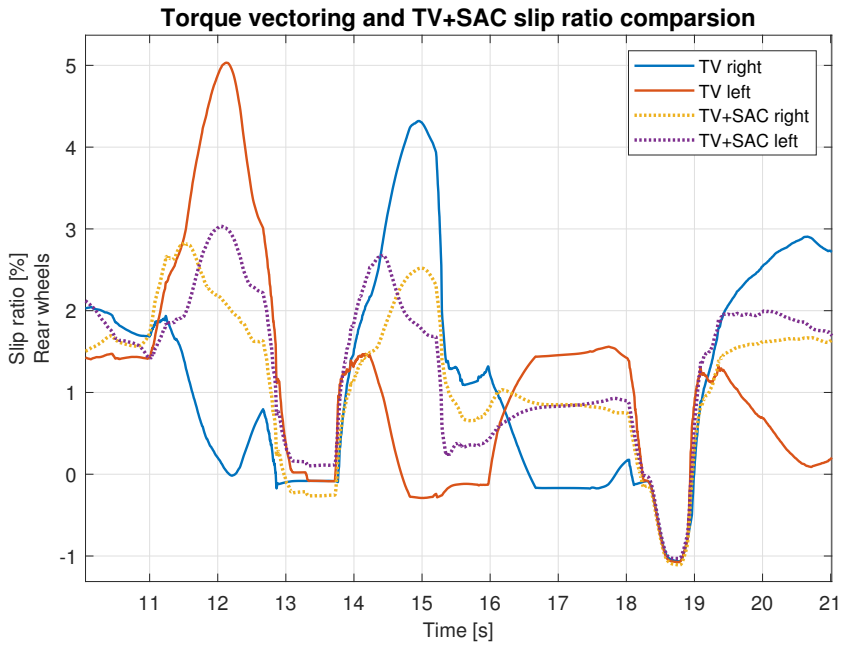

Figure 5.7: Slip ratio values on rear wheels during the simulation in IPG Carmaker. Comparison of algorithms TV and TV with steering angle control is drawn.

For clarity it is stated only short interval form previous Figure 5.6 (development of other variables is on that figure). It is apparent that slip ratios of algorithm TV+SAC don't reach high values as it is in case of algorithm TV. This can be a big benefit in given situations.

Chapter 6

Experimental Results

6.1 Student Formula

Algorithms were tested and validated on student formula in cooperation with eForce FEE Prague Formula.

Figure 6.1: Student formula created by eForce FEE Prague formula. Algorithms were tested on this formula.

In formula devices are connected and data are send by CAN bus. In formula Inertial measurement unit, Vehicle dynamics control unit, Motor control unit and other systems units are implemented. By using them it is possible to

obtain all the needed data. They provide necessary information about vehicle velocity, $\dot{\psi}$, β, ω, $v_{xf,xr}$, steering wheel angle, τ and many others. Faulty measurement of any signal is indicated by relevant valid signal. In the tested day variable β was faulty (almost the whole time). Thus, controller β was turned off by signal β_{valid} during most of the measurement time. Therefore it's not shown on following figures.

CAN bus in formula run on frequency f=100 Hz. It is possible in Carmaker to run simulation in option discrete time. So algorithms were tested on this frequency to validate their functionality. They were slightly modified by discrete design. 100 Hz is sufficient in simulation, but in the formula it is not ideal. Better measurement could be performed on higher sample frequency.

This frequency don't causes a problem for the most of signals, but slip ratio measurement (based on circumferential wheel velocity) would have smoother development. Slip ratio measurement has also another problem: it is not enough precise. According to Eq. 2.2 circumferential wheel velocity measurement deviation 0.05 m/s at longitudinal wheel speed $v_x = 10$ m/s creates 0.5% slip ratio measurement error. That is too much for torque vectoring with slip ratio control functionality. Furthermore it can occur on both tires at the same time. Figure 6.2 show slip ratio measurement on formula without TV functionality.

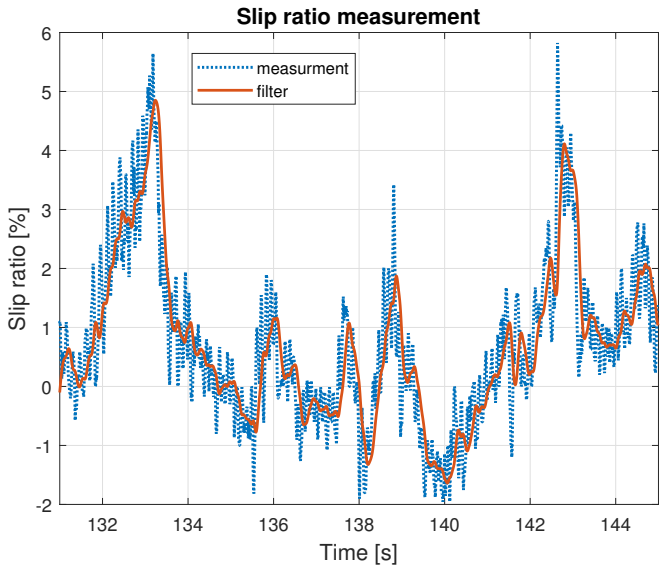

Figure 6.2: Slip ratio on rear wheels development during the drive test on formula. Big noise causes inaccuracy. Filter was implemented.

This figure shows slip ratio measurement noise. Low pass filter on 15 Hz

was implemented. It suppresses this measurement noise, but regrettably, the filter causes signal delay. (It is not apparently from the figure, but 0.1 s is too much.) Unfortunately solution of this problem wasn't achieved. Various filters were implemented, but they either didn't give acceptable results about noise reduction or they delayed the signal too much. From this reason algorithm TV with slip ratio control can't work on formula.

6.2 Drive Tests

Next results based on drive test are achieved with TV without slip ratio control.

Here, several results from drive test on formula will be shown. Dynamics of formula was improved in all of this cases. Presented figures can't describe driver's feelings during the drive and all improved drive ability. Despite of this luck driver's feelings are the only objective way of designed algorithm evaluation. Comparison between drive test with and without torque vectoring is stated below. Similar inputs (mainly steering angle δ_f) to system for similar formula speeds with TV and without TV were found.

Stated above, side slip angle wasn't valid during drive test with TV (almost the whole time), therefore it won't be shown in figures.

The first graph (Figure 6.3) from drive tests compare yaw rate response to steering angle step at 16 m/s.

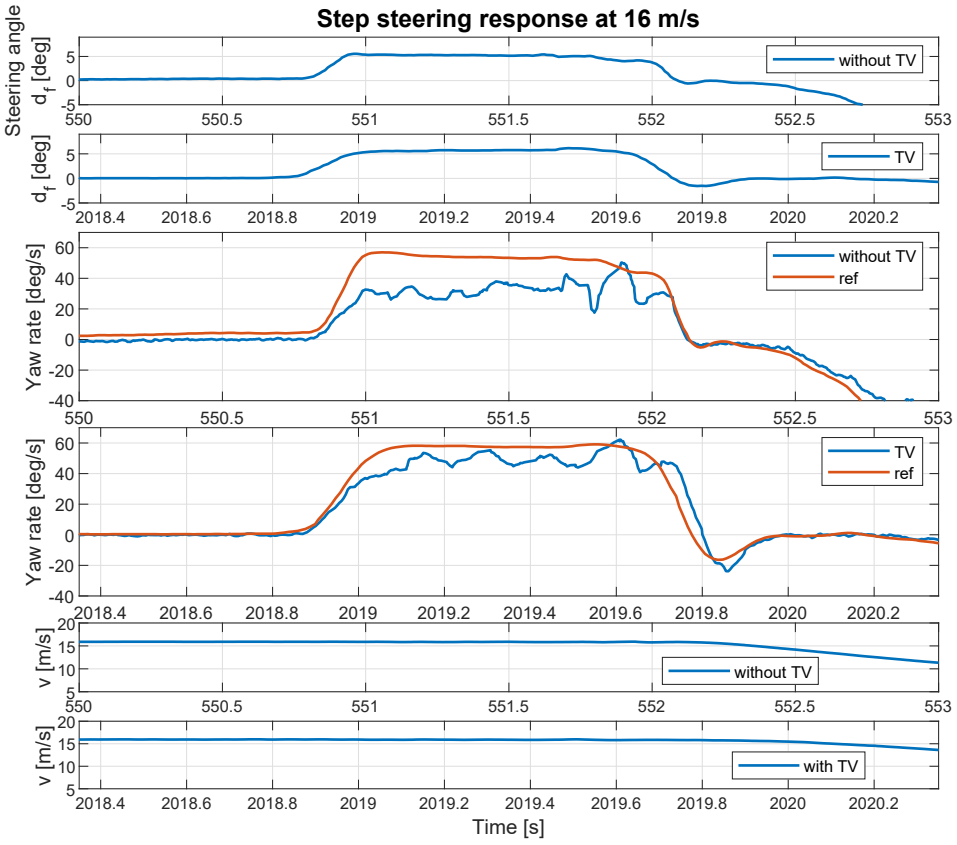

Figure 6.3: Yaw rate response to steering angle step at 16 m/s. Comparison of variables values development with and without TV.

It is clear, that formula dynamics with TV track the reference vehicle better. That's obvious that yaw rate oscillations isn't caused by TV, but it's presented also without TV. Another comparison was performed again at 16 m/s.

On Figure 6.4 are two ramps and recorded are also variables values development between them.

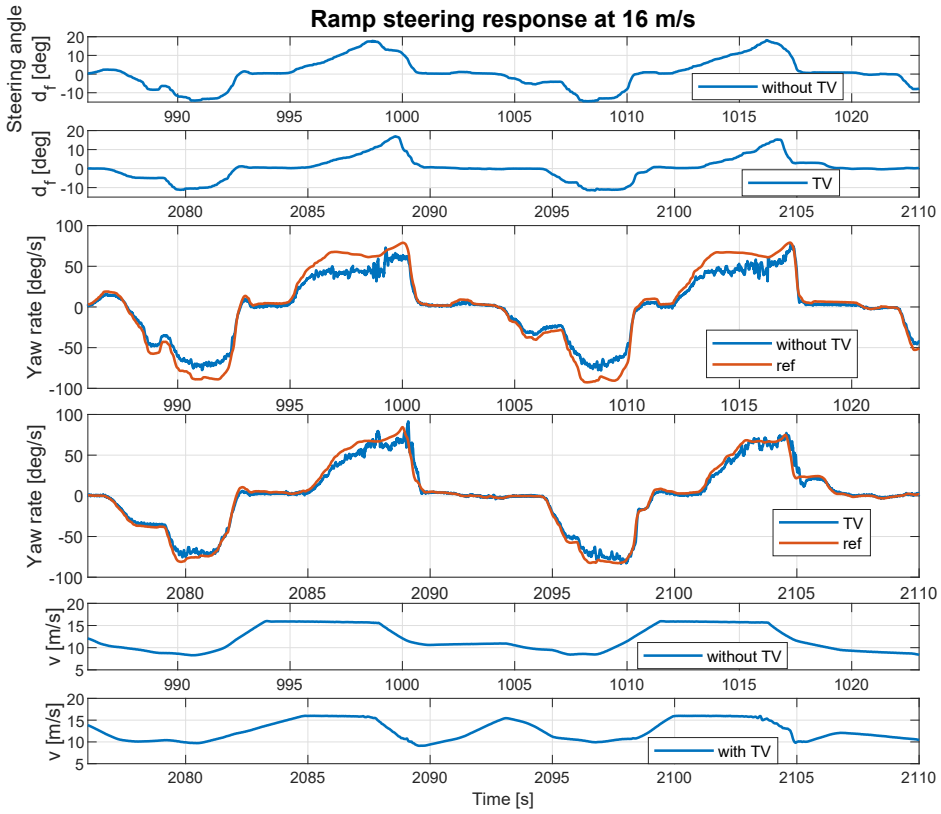

Figure 6.4: Yaw rate response to ramp steering angle at 16 m/s. Comparison of variables values development with TV and without TV.

The first ramp starts at time 995 s (2085 s), the second one at 1012 s (2100 s). Improved drive abilities are apparent. Also variable value course between these ramps supports it.

Last comparison was carried out at speed 20 m/s. On Figure 6.5 is presented step steering angle response.

Figure 6.5: Yaw rate response to step steering angle at 20 m/s. Comparison of variables values development with TV and without TV.

Also in this case is formula behavior less understeer. At first it almost tracks the reference vehicle $\dot{\psi}$ value. Initially step response is quite fast. Slight delay follows on step down (approximately 0.07 s). But that's sporadic case that causes proposed control only partially (similar development, but in smaller amount, can be noticed in Figure 6.3) and there might be also other factors.

Chapter 7

Conclusion and Future Work

In Chapter 2 was adopted, described and modified single-track vehicle model to triple-track model with two rear wheels and one front wheel, so it could be used for torque vectoring and torque vectoring with slip ratio control. Next tire modelling is described. In following Chapter 3 vehicle stability is analysed and performed brief analysis of drive ability of formula as understeering vehicle. The main aim of this thesis was to design control algorithm for torque vectoring without and with longitudinal slip ratio control. This is done in Chapter 4. Functionality and action principles of these algorithms are validated in following Chapters 5, 6 by drive test in simulation environment IPG Carmaker and drive test with electric formula. Unfortunately it was impossible to validate algorithm based on slip ratio control within formula drive tests. The reason was imprecise measurement of this variable, As implemented filters didn't improve this measurement. However, benefits of this approach is obvious from simulation and by comparison with torque vectoring without slip ratio control.

Tire slip angle wasn't controlled in this thesis and there were neglected several impacts that affect the vehicle dynamics. Feasible control of front wheels steering angle is shown in this thesis. There is big potential at controlling vehicle's rear wheels. Automotive industry offers many options and new approaches. Some of these possibilities I would like to investigate in my future master education.

Appendix A

Bibliography

[1] Denis Efremov. Unstable ground vehicles and artificial stability systems. Master's thesis, Czech Technical University in Prague, Faculty of Electrical Engineering, Praha, 2018.

[2] Denis Efremov, Tomáš Haniš, and Martin Hromčík. Introduction of driving envelope and full-time-full-authority control for vehicle stabilization systems. *IEEE Xplore*, 2019.

[3] T. D. Gillespie. *Fundamentals of Vehicle Dynamics*. Society of Automotive Engineers, Warrendale, PA, c1992.

[4] IPG AUTOMOTIVE GmbH, c2019. Accessed: 2019-04-24. URL: `https://ipg-automotive.com/`.

[5] Lukáš Haffner. *Real-time tire models for lateral vehicle state estimation*. Phd thesis, Technischen Universität Wien, Fakultät für Maschninenbau, Wien, 2008.

[6] U. Kiencke and Lars Nielsen. *Automotive control systems*. Springer, Berlin, 2nd edition, c2005.

[7] Marek Lászlo. Flight control solutions applied for improving vehicle dynamics. Master's thesis, Czech Technical University in Prague, Faculty of Electrical Engineering, Praha, 2019.

[8] Douglas L. Milliken and William F. Milliken. *Race car vehicle dynamics*. SAE International, Warrendale, PA, c2003.

[9] Martin Mondek. Active torque vectoring systems for electric drive vehicles. Master's thesis, Czech Technical University in Prague, Faculty of Electrical Engineering, Praha, 2018.

[10] Hans B. Pacejka. *Tire and Vehicle Dynamics*. SAE International, 2nd edition, 2005.

[11] Dieter Schramm, Manfred Hiller, and Roberto Bardini. *Vehicle dynamics*. Springer, New York, 2014.

Appendix B

List of abbreviations, symbols and parameters

- **Abbreviations**

ABS	Anti-lock Braking System
ESP	Electronic Stability Program
TC	Traction Control
TV	Torque Vectoring
SAE	Society of Automotive Engineers
CoG	Centre of Gravity
CoP	Centre of Pressure
PID	Proportional–Integral–Derivative Controller
TV SC	Torque Vectoring with Slip Ratio Control
TV+SAC	Torque Vectoring with Steering angle Control

Symbols

α	tire slip angle
β	vehicle side slip angle
C_f	front tire stiffness coefficient
C_r	rear tire stiffness coefficient
δ_f	front wheels steering angle
f	front
F_x	longitudinal force
F_y	lateral force
F_z	vertical force
F_{x_aero}	longitudinal drag force
F_{z_aero}	vertical pressure force
K	understeering gradient
M_z	self-aligning moment
μ	road friction coefficient
λ	longitudinal slip ratio
τ_f	front wheels torque
τ_r	rear wheels torque
τ_{bf}	front wheels brake torque
τ_{br}	rear wheels brake torque
v	velocity
v_x	longitudinal velocity
v_y	lateral velocity
ω	wheel angular speeds
r	rear
$r1$	rear right wheel
$r2$	rear left wheel
$\dot{\psi}$	vehicle yaw rate

Parameters

Description	Notation	Value
Vehicle mass	m	285 kg
Vehicle vertical axis moment of inertia	I_z	120 kgm^2
Vehicle wheel base	w	1.54 m
Vehicle rear track	tr	1.296 m
Longitudinal distance of front axle from center of gravity	l_f	0.72 m
Longitudinal distance of rear axle from center of gravity	l_r	0.82 m
Longitudinal distance of front axle from center of pressure	l_{fp}	0.86 m
Longitudinal distance of rear axle from center of pressure	l_{rp}	0.68 m
Lift coefficient of vehicle body related to center of pressure	C_L	-3.5
Drag coefficient of vehicle body related to center of pressure	C_D	-1.3
Aerodynamic reference area	S	1.19 m
Air density	ρ	1.225 kgm^3

Table B.1: Formula parameters (adopted from [7]).

Description	Notation	Value
Tire radius	R	0.2 m
Front tire moment of inertia	J_f	0.1381 kgm^2
Rear tire moment of inertia	J_r	0.1376 kgm^2
Longitudinal shape factor	C_x	1.4
Longitudinal peak factor	D_x	1.4
Longitudinal stiffness factor	B_x	0.165
Longitudinal curvature factor	E_x	-1
Lateral shape factor	C_y	1.45
Lateral peak factor	D_y	1.4
Lateral stiffness factor	B_y	0.184
Lateral curvature factor	E_y	-0.3
Lateral self aligning factor	C_z	3.75
Lateral self aligning factor	D_z	-0.03
Lateral self aligning factor	B_z	0.11
Lateral self aligning factor	E_z	0.9

Table B.2: Formula tire parameters (adopted from [7]).

Appendix C

Content of enclosed CD

- This thesis in pdf format,
- Source files,
- Measured data.